Title

Bitopic Sphingosine 1-Phosphate Receptor 3 (S1P3) Antagonist Rescue from Complete Heart Block: Pharmacological and Genetic Evidence for Direct S1P3 Regulation of Mouse Cardiac Conduction

Journal

Molecular Pharmacology, 89(1)

ISSN

0026-895X

Authors

Sanna, M Germana
Vincent, Kevin P
Repetto, Emanuela
et al.

Publication Date

2016

DOI

10.1124/mol.115.100222

Peer reviewed

1521-0111/89/1/176–186$25.00
MOLECULAR PHARMACOLOGY

http://dx.doi.org/10.1124/mol.115.100222
Mol Pharmacol 89:176–186, January 2016

Bitopic Sphingosine 1-Phosphate Receptor 3 (S1P3) Antagonist Rescue from Complete Heart Block: Pharmacological and Genetic Evidence for Direct S1P3 Regulation of Mouse Cardiac Conduction

M. Germana Sanna,[1] Kevin P. Vincent,[1] Emanuela Repetto,[1] Nhan Nguyen, Steven J. Brown, Lusine Abgaryan, Sean W. Riley, Nora B. Leaf, Stuart M. Cahalan, William B. Kiosses, Yasushi Kohno, Joan Heller Brown, Andrew D. McCulloch, Hugh Rosen, and Pedro J. Gonzalez-Cabrera

Departments of Chemical Physiology (M.G.S., E.R., N.N., H.R., P.J.G.-C.), Immunology (N.B.L.), and Molecular and Cellular Neuroscience (S.M.C.), Scripps Research Institute Molecular Screening Center (S.J.B., L.A., S.W.R.), Microscopy Core (W.B.K.), Scripps Research Institute, La Jolla, California; Kyorin Pharmaceutical Company, LTD, Tokyo, Japan (Y.K.); and Departments of Bioengineering (A.D.M., K.P.V.) and Pharmacology, University of California, San Diego, California (J.H.B.)

Received June 8, 2015; accepted October 20, 2015

ABSTRACT

The molecular pharmacology of the G protein–coupled receptors for sphingosine 1-phosphate (S1P) provides important insight into established and new therapeutic targets. A new, potent bitopic $S1P_3$ antagonist, SPM-354, with in vivo activity, has been used, together with $S1P_3$-knockin and $S1P_3$-knockout mice to define the spatial and functional properties of $S1P_3$ in regulating cardiac conduction. We show that $S1P_3$ is a key direct regulator of cardiac rhythm both in vivo and in isolated perfused hearts. 2-Amino-2-[2-(4-octylphenyl)ethyl] propane-1,3-diol in vivo and S1P in isolated hearts induced a spectrum of cardiac effects, ranging from sinus bradycardia to complete heart block, as measured by a surface electrocardiogram in anesthetized mice and in volume-conducted Langendorff preparations. The agonist effects on complete heart block are absent in $S1P_3$-knockout mice and are reversed in wild-type mice with SPM-354, as characterized and described here. Homologous knockin of $S1P_3$-mCherry is fully functional pharmacologically and is strongly expressed by immunohistochemistry confocal microscopy in Hyperpolarization Activated Cyclic Nucleotide Gated Potassium Channel 4 (HCN4)-positive atrioventricular node and His-Purkinje fibers, with relative less expression in the HCN4-positive sinoatrial node. In Langendorff studies, at constant pressure, SPM-354 restored sinus rhythm in S1P-induced complete heart block and fully reversed S1P-mediated bradycardia. $S1P_3$ distribution and function in the mouse ventricular cardiac conduction system suggest a direct mechanism for heart block risk that should be further studied in humans. A richer understanding of receptor and ligand usage in the pacemaker cells of the cardiac system is likely to be useful in understanding ventricular conduction in health, disease, and pharmacology.

Introduction

Five high-affinity G protein–coupled receptors for sphingosine 1-phosphate (S1P) have been identified (Rosen et al., 2013), and the crystal structure of $S1P_1$ has been solved (Hanson et al., 2012). This receptor cluster is medically important because the nonselective Sphingosine 1-Phosphate receptor (S1P-R; $S1P_1$, $S1P_3$, $S1P_4$, and $S1P_5$) modulator prodrug fingolimod [2-amino-2-[2-(4-octylphenyl)ethyl]propane-1,3-diol (FTY720)] is an effective oral therapy for the treatment of relapsing, remitting multiple sclerosis by altering lymphocytic and central functions (Cohen et al., 2010; Kappos et al., 2010). Five ($S1P_{1–5}$) subtypes that differ in spatial distribution, coupling, and function can, singly or in combination, play complex roles in the embryonic formation of the arterial media, blood pressure regulation, and cardiac function [reviewed by Mendelson et al. (2014)]. For example, FTY720 in humans is associated with significant sinus bradycardia and prolongation of the QTc interval (Schmouder et al., 2006; Kappos et al., 2010; Espinosa and Berger, 2011; Yagi et al., 2014). FTY720 treatment has additionally revealed an

This work was supported by the National Institutes of Health [Grant 5U54 MH084512 to H.R. and Grants 1RO1HL105242 and 1R03EB014593 to A.D.M] and Kyorin Pharmaceuticals [Grant SFP-1499 to H.R.].
[1]M.G.S., K.P.V., and E.R. contributed equally to this work.
dx.doi.org/10.1124/mol.115.100222.
This article has supplemental material available at molpharm.aspetjournals.org.

ABBREVIATIONS: AV, atrioventricular; AVN, atrioventricular node; bpm, beats per minute; CCS, cardiac conduction system; CF, coronary flow; CHB, complete heart block; ECG, electrocardiogram; FTY720, 2-amino-2-[2-(4-octylphenyl)ethyl]propane-1,3-diol; HCN4, cyclic nucleotide-gated K^+ channel 4; IHC, immunohistochemistry; KI, knockin; KO, knockout; PBS, phosphate-buffered saline; PBST, phosphate-buffered saline + 0.5% Triton X-100; PCR, polymerase chain reaction; RT, room temperature; SAN, sinoatrial node; S1P, sphingosine 1-phosphate; WT, wild type.

increased incidence of atrioventricular (AV) disturbances during the first dose, including AV block and asystole, particularly in subgroups of patients with preexisting cardiac conditions that require other therapeutics, i.e., beta blockers and calcium channel blockers, to maintain adequate cardiovascular dynamics (Vanoli et al., 2014). Atropine reversal of the sinus bradycardia (Kovarik et al., 2008) and the demonstration of sinus bradycardia with $S1P_{1/5}$-selective agonists in humans (Legangneux et al., 2013) as well as rodents (Fryer et al., 2012) suggest that sinoatrial node (SAN) effects and those events resulting from alterations in AV-nodal conduction might be distinctly regulated.

There is little evidence to date concerning actual protein expression for the distinct S1P-R subtypes in the mammalian cardiac conduction system (CCS), a highly differentiated, neural-crest derived system responsible for initiating (SAN) and propagating [atrioventricular node (AVN) and His-Purkinje system] synchronous cardiac contractions. Pharmacologically, S1P-R activation by S1P, FTY720, and selective $S1P_{1/5}$ agonists all induce cardiac depression, both at the level of the SAN (Guo et al., 1999) as well as by activating cardiomyocyte $S1P_1$ G protein-coupled inwardly-rectifying potassium channel currents (Bunemann et al., 1995; Fryer et al., 2012; Legangneux et al., 2013). At the AVN level, in rats, FTY720 was recently shown to elevate the PR-interval duration or total AV conduction time, which defines first-degree AV block (Egom et al., 2015). In the same study, the authors also demonstrated the presence of $S1P_{1–3}$ transcripts in AVN, suggesting a direct link between FTY720's PR-interval augmentation and $S1P_{1–3}$ engagement in situ.

The analysis of in vivo $S1P_3$ cardiac function can be confounded by its high expression on vascular smooth muscle (Forrest et al., 2004), where, functionally, it can result in vasoconstriction to S1P (Salomone et al., 2003, 2008) or, in the case with FTY720, an acute overall increase in total peripheral resistance (Fryer et al., 2012). Consistent with the role of $S1P_3$ in vasoconstriction, Murakami et al. (2010) demonstrated that the coronary flow (CF) rate reduction observed following S1P perfusion in rat Langendorff heart preparations was fully sensitive to $S1P_3$ antagonist reversal.

The detailed understanding of $S1P_3$ signaling in the CCS remains incomplete. We have approached the problem of defining receptor usage in distinct and highly differentiated cell populations that are difficult to study ex vivo by building a tool set of both genetic and pharmacological tools that together define $S1P_3$ distribution and function. In this report, we characterize a novel bitopic $S1P_3$ antagonist, SPM-354, which competes for binding in both the orthosteric and allosteric sites, as defined by the natural ligand and the selective allosteric $S1P_3$ agonist CYM-5541, respectively (Parrill et al., 2000; Schürer et al., 2008; Jo et al., 2012). Using SPM-354, the $S1P_1$ selective antagonist W146 (Sanna et al., 2006), and fluorescence-tagged $S1P_3$-mCherry knockin (KI) mice in concert with the previously described $S1P_3$-knockout (KO) mouse (Ishii et al., 2001; Yang et al., 2002), we combined these systems to allow the roles of $S1P_3$ causal expression and its functional consequences in the CCS to be more clearly defined.

Materials and Methods

Synthesis of SPM-354. SPM-354 was synthesized as follows: 122 mg, 0.164 mmol (Supplemental Fig. 1) was dissolved in MeCN (2 ml), and iodotrimethylsilane (117 μl, 0.822 mmol) was slowly added at 0°C under an argon atmosphere. After stirring for 30 minutes at 0°C, the reaction mixture was poured into water (10 ml), and then the resultant mixture was stirred for 1 hour at 0°C. The precipitate was filtered, washed with water, and dried in vacuo at 50°C. The crude residue was dissolved in MeOH and stirred for 30 minutes at RT (room temperature), and then the mixture was filtered and insoluble materials were washed with MeOH (5 ml). The filtrate was concentrated in vacuo. The residue was suspended in MeCN and stirred for 30 minutes at RT, and then the resultant precipitate was filtered, washed with MeCN, and dried in vacuo at 50°C to give SPM-354 (50 mg, 0.0973 mmol) as a colorless powder (m.p.: 156–159°C). [α]D25: −7.67 (c 0.50, MeOH). ^{1}H NMR (dimethylsulfoxide-d6-dTFA, 400 MHz):δ 0.90 (3H, t, J = 7.3 Hz), 1.26–1.40 (2H, m), 1.54–1.66 (2H, m), 1.70–1.82 (2H, m), 2.61–2.75 (2H, m), 3.86–3.97 (2H, m), 7.10 (1H, d, J = 7.9 Hz), 7.19 (1H, dd, J = 7.9, 1.8 Hz), 7.27 (1H, d, J = 1.8 Hz), 7.34 (1H, d, J = 7.9 Hz), 7.40 (1H, d, J = 1.8 Hz), and 7.56 (1H, d, J = 8.6 Hz). high-resolution electrospray ionisation mass spectrometry (+): 514.08255 (calculated for C20H25ClF3NO5PS, 514.08317). Analysis calculated for C20H24ClF3NO5PS. 0.1H2 O: C, 46.74%; H, 4.71%; and N, 2.73%. Found: C, 46.58%; H, 4.73%; and N, 2.72%. SPM-354 is reference example 47 in WO2011004604 (Yasushi et al., 2011).

SPM-354 Selectivity. Receptor activation through beta-arrestin recruitment (TANGO; Life Technologies, Carlsbad, CA) was used to determine SPM-354 selectivity. U2OS cells stably expressing individual S1P receptors ($S1P_{1–5}$) were seeded on 384-well plates at 10,000 cells per well and incubated for 48 hours according to the manufacturer's protocol. SPM-354 in 1% fatty acid free bovine serum albumin was added at the indicated concentrations to incubate for 1 hour. The S1P or selective $S1P_3$ agonist CYM-5541 concentrations were added to the wells and incubated for 4 hours at 37°C, followed by the addition of the LiveBLAzer reagent. Following 2 hours, the plates were read on an EnVision (Perkin Elmer, Waltham, MA) plate reader to measure S1P or CYM-5541 activity, blue (410 nm excitation, 460 emission) to green (410 excitation, 535 emission), ratios. For Schild analyses in $S1P_1$ and $S1P_3$ cells, the S1P or CYM-5541 concentration response curves were fit using sigmoidal nonlinear regression in GraphPad Prism software (GraphPad Software, Inc., La Jolla, CA), and the resulting EC_{50} values were compared with no-ligand controls to generate the dose ratios. These were graphed in the Schild's plot versus the log [M] of SPM-354, yielding the pA_2 values.

Animals. Experiments were conducted in accordance with the National Institutes of Health Guide for the Care and Use of Laboratory Animals, following approved protocols by the Institutional Animal Care and Use Committee at the Scripps Research Institute (La Jolla, CA) and the University of California, San Diego. Wild-type (WT) C57BL/6J male mice were obtained from the Scripps Research Institute in-house breeding colony. Experiments with KO and KI mice included 8–12 week old male, C57BL/6J background animals bred for at least 20 generations. Isolated heart experiments were conducted with 8–12 week old male C57BL/6J mice and obtained from the Jackson Laboratory (Bar Harbor, ME) and age-matched male KO mice.

In Vivo Electrocardiogram Recordings. Electrocardiograms (ECGs) were recorded in Avertin (240 milligram per kilogram (mpk) i.p.) anesthetized mice using subcutaneous inserted electrodes. Recordings were performed on a PowerLab 8/35 (AD Instruments, Dunedin, New Zealand) data acquisition unit at a 4-kHz sampling rate and under a heat lamp. Reversal of single-dose FTY720-induced bradycardia by SPM-354 was assessed in mice preadministered i.p. with 20 mpk FTY720 for 5 hours, following anesthesia and a baseline ECG period of 4–6 minutes. After baseline determination, mice were challenged i.p. with either 40 mpk SPM-354 or vehicle (20% β-cyclodextrin; Sigma Aldrich, St. Louis, MO), with continuous recording until 12 minutes. For determination of the RR- and PR-interval duration, we included those values at the end of baseline equilibration with those at the end of FTY720 treatment taken from LabChart Pro software (AD Instruments).

For FTY720 complete heart block (CHB) reversal experiments, WT mice pretreated with 20 mpk FTY720 for 5 hours were anesthetized as above, implemented for ECG recording, and challenged at the onset of the appearance of consecutive P-waves without a sequential QRS complex, with either 80 mpk SPM-354 i.p. or 1 mpk atropine, and recorded further to 12 minutes.

For FTY720-propranolol CHB experiments, WT, KI, or KO mice were pretreated with 20 mpk FTY720 for 5 hours and challenged with 1 mpk (*S*)-(−)-propranolol (Sigma Aldrich) during the last hour of FTY720 incubation. Two minutes prior to anesthesia, mice were then treated i.p. with a single 120-mpk dose of SPM-354 or an equal volume of vehicle, and ECG recordings were further collected for 12 minutes.

Data are shown as the mean ± S.E.M. Statistical analyses between conditions were done using unpaired, two-tailed *t* tests (95% confidence interval) or two-way repeated-measure analyses of variance followed by a Bonferroni test (GraphPad Prism; GraphPad Inc.).

Isolated Heart Studies. For volume-conducted ECG studies, WT or $S1P_3$-KO mouse hearts were excised from mice anesthetized with 2.5% isoflurane in 100% oxygen. After aortic cannulation, the hearts were perfused retrograde with a constant pressure (70 mm Hg) Langendorff setup using 37°C heated, oxygenated Krebs-Henseleit solution, as reported (Liao et al., 2012). The hearts were placed in a custom chamber containing 37°C warmed perfusate with two electrodes and a ground lead for the recording of volume-conducted ECG. The voltage signal was filtered and amplified, and 60-Hz noise was removed (Hum Bug Noise Eliminator; Quest Scientific, North Vancouver, Canada) before the signal was digitized at 5000 Hz. Parallel measurements of the CF rate were made using an in-line flow probe (Transonic Systems, Inc., Ithaca, NY), and the average flow rate (0.1 Hz low-pass filtered) was recorded. Volume-conducted ECG and coronary flow rate data were analyzed with custom software in MATLAB (MathWorks, Natick, MA). ECGs were further digitally filtered (250 Hz low pass) for display.

Drug delivery from a 0.5 mg/ml stock of S1P (Avanti Polar Lipids, Inc., Alabaster, AL) in 50 mM Na_2CO_3–20% β−cyclodextrin, 5 mg/ml SPM-354 stock in 20% β-cyclodextrin, 1 mg/ml W146 (Avanti Polar Lipids, Inc.) in 50 mM Na_2CO_3–20% β−cyclodextrin, or 1 mM atropine (Sigma Aldrich) was done by dissolving stocks into 3–5 ml volumes of a prewarmed, gassed Krebs-Henseleit solution to be delivered to the perfusion line.

Generation of $S1P_3^{mCherry/mCherry}$ Mice. Both the 5′ (4.5 kilobase) and 3′ (3.5 kilobase) arms of Exon2 encoding for the mouse *S1pr3* gene were cloned by polymerase chain reaction (PCR) from BAC (RP24-69B23, C.H.O.R.I) into the Psp72 backbone vector (Promega, Madison, WI) and sequenced. mCherry (Clontec, Mountain View, CA) and the loxP neomycin resistance cassette (CAN; a generous gift from Mario Capecchi) were subsequently added downstream from the coding sequence of *S1pr3.* The linearized construct was injected into clone Bruce4 embryonic stem cells derived from C57BL/6J mice. Homologous recombination was confirmed by Southern blot using two different 5′ probes. Correctly targeted C57BL/6J embryonic stem cells were injected into recipient C57BL/6J (B6 albino) blastocysts. The resulting chimeric animals were crossed to C57BL/6J mice. Heterozygotes were mated to generate homozygous mice. Genotyping was performed from genomic DNA extracted from tails by PCR using two reverse and a common forward primer. PCR was performed using Phire polymerase (NEB) with two reverse primers (BW) and a common forward primer: P mCherry N1 686 BW, 5′ TCA CCA TGG TGG CGA CCG GTG GCT TGC A 3′; S1pr3 11322 BW, 5′ AGG CTG AAA TGC GTT GGT GAC TCC TTG GGT 3′; and S1pr3 11103 forward primer, 5′ ATG CAG CCT GCC CTC GAC CCA AGC AGA AGT 3′. All mice used were between 8 and 12 weeks of age. $S1P_3^{mCherry/mCherry}$ mice were then crossed onto the $S1P_1^{eGFP/eGFP}$ mice strain (Cahalan et al., 2011) to generate the double homozygote mouse line $S1P_3^{mCherry/mCherry}$/$S1P_1^{eGFP/eGFP}$.

Generation of Anti–mCherry Monoclonal Antibody for Western Blottings and Immunohistochemistry. Rat anti-mouse mCherry was generated at the Scripps Research Institute Center for Antibody Development and Production by i.p. immunization of Wistar rats with 50 μg of mCherry fluorescent protein (Biovision, Milpitas, CA) in 200 μl of phosphate-buffered saline (PBS)/Sigma Adjuvant System (Sigma Aldrich) and two antigen boosts in PBS/adjutant 3 weeks apart. Antigen-positive hybridomas were expanded, and a clone, 16D7, was isolated after three rounds of limited dilution subcloning. Antibodies were further purified by protein G chromatography. Clone 16D7 rat anti-mCherry antibody is commercially available at Life Sciences (Carlsbad, CA) and Kerafast (Boston, MA).

$S1P_3$-mCherry Expression via Western blotting. Excised whole hearts from homozygous $S1P_3$-KI mice or $S1P_3$-KO mice were rinsed in cold PBS, minced, and homogenized in RIPA buffer with the HALT protease inhibitor cocktail (Thermo Scientific Pierce Protein Research Products, Waltham, MA). Lysate processing, protein determination, SDS-PAGE, and blotting were performed as reported by Cahalan et al. (2011). $S1P_3$-mCherry expression was detected using 30 μg of protein per lane with the anti-mCherry primary (1:1000) described above, followed by rat HRP secondary (Jackson ImmunoResearch Inc., West Grove, PA) with ECL Plus (GE Healthcare Bio-Sciences, Pittsburgh, PA).

Perfusion, Tissue Sectioning, and Immunohistochemistry of Mouse Heart. Sample preparation for staining was performed as follows: mice were euthanized by CO_2 asphyxiation and perfused through the heart with Z-fix (Anatech LTD, Battle Creek, MI). Hearts were harvested and fixed in Z-fix for 1 hour and placed into a 30% sucrose/PBS solution for 48 hours at 4°C. Samples were frozen in blocks of optimal cutting temperature (Tissue Tek) with dry ice and ethanol. 40 to 100 μm sections were cut using a Microtome (Microm HM 550; ThermoFisher Scientific, Waltham, MA). Immunohistochemistry (IHC) sections were permeabilized in PBS + 0.5% Triton X-100 (PBST) for 2 hours at RT, blocked in PBST for 2 hours at RT with 5% normal goat serum, washed three times in PBST, and incubated for 12 hours at 4°C with primary antibody (1:100) diluted in PBST + 1% normal goat serum. Primary incubation was followed by washing (three times) in PBST, incubated with secondary antibody in PBST at 1:1000 dilution for 2 hours at RT, washed three times in PBS, stained for 1 hour with DAPI (1:500), and mounted on Vectashield (Vector Laboratories, Burlingame, CA) for confocal microscopy. The following primary antibodies were used for staining: anti-mCherry, anti-green fluorescent protein (GFP) (Abcam, Cambridge, UK), CD31 (Abcam), cyclic nucleotide-gated K^+ channel 4 [HCN4 (cyclic nucleotide-gated K^+ channel 4)] (Santa Cruz Biotechnology, Dallas, TX), and Pan-Neuronal (Millipore, Darmstadt, Germany). Secondaries were Alexa 555, Alexa 633, Phalloidin 488, and 4′,6-diamidino-2-phenylindole-nuclear stain (Life Technologies).

Confocal Microscopy. Confocal images were obtained with a Zeiss LSM 780 laser scanning confocal microscope and processed with Zen 2012 software (both Carl Zeiss Inc., San Diego, CA). Z stacks of images (obtained at 0.3-μm optical slice increments) were collected sequentially using a 63× objective and then were maximum projected into single flattened stacks for figure panels. In some cases, Z stacks were additionally imported into IMARIS software (Bitplane Inc., Concord, MA) for three-dimensional rendering.

Results

SPM-354 Ligand. SPM-354 (Fig. 1A), a 2-propyl substituent of the previously described $S1P_3$ antagonist SPM-242 (Jo et al., 2012), was found to be 6- to 10-fold more potent than SPM-242 for antagonizing S1P-$S1P_3$ β-arrestin recruitment (Supplemental Fig. 2A) and 30-fold more potent on $S1P_3$ versus $S1P_1$ (Supplemental Fig. 2B). In $S1P_3$ cells and similar to the bitopic antagonist SPM-242, SPM-354 was shown to be noncompetitive against the selective allosteric $S1P_3$ agonist CYM-5541 (estimated equilibrium dissociation constant = −9.01 ± 0.45;

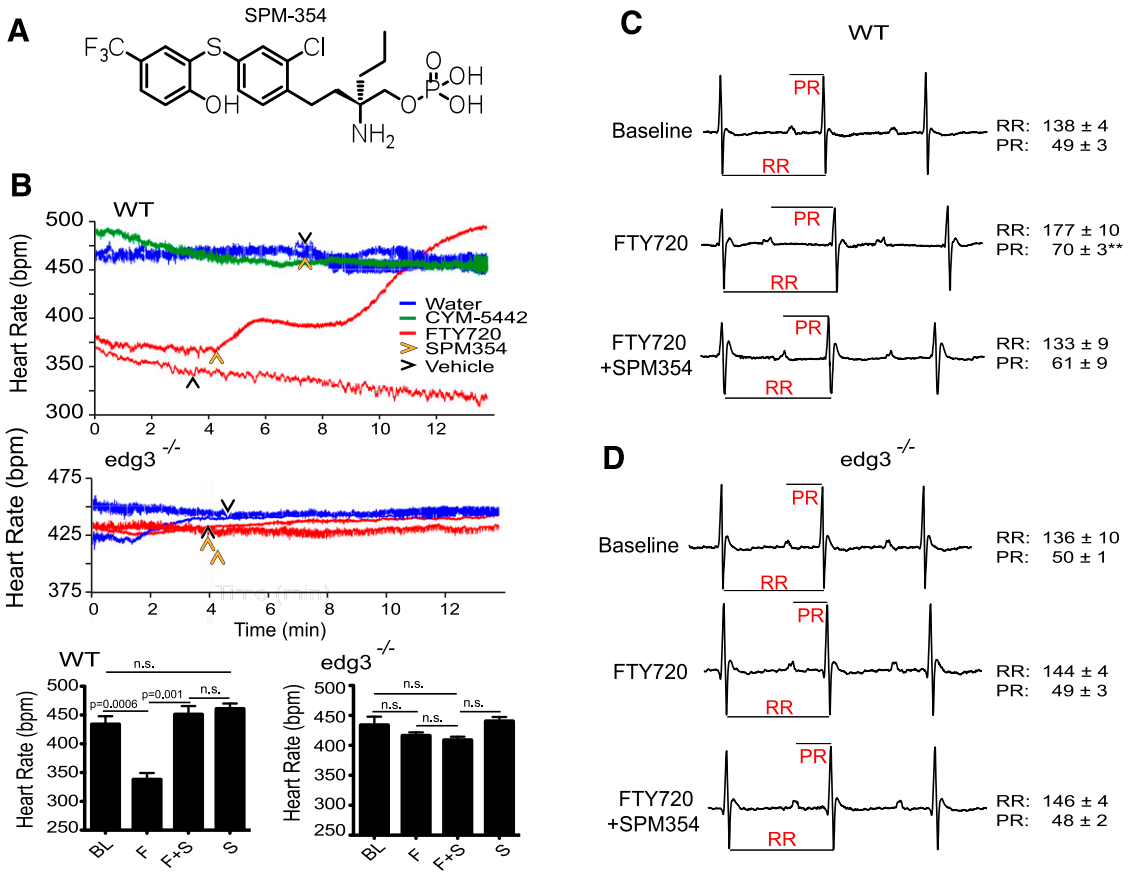

Fig. 1. S1P$_3$-dependent bradycardia by FTY720 treatment is associated with enhanced RR- and PR-interval duration that is reversed by SPM-354. (A) Chemical structure of SPM-354. (B) Typical chronotropic responses in WT mice following 5-hour treatment with vehicle, FTY720, or the S1P$_1$ agonist CYM-5442. The recordings show that a single i.p. SPM-354 dose, but not antagonist vehicle, fully reverses FTY720-mediated bradycardia without having a significant effect on heart rate when administered alone. The top graph shows that CYM-5442 does not significantly alter heart rate in WT mice at 5 hours postadministration. Absence of bradycardia by FTY720 in S1P$_3$ KO mice (lower graph). Bar graphs show the mean ± S.E.M. heart rates in WT and S1P$_3$ KO mice throughout baseline (BL), FTY720 (F), FTY720 + SPM-354 (F+S), or SPM-354 alone (S) conditions. Electrocardiographic waveforms in FTY720-treated mice display enhanced RR- and PR-interval duration in wild-type (C) but not S1P$_3$ KO (D) mice and partial restoration upon SPM-354 administration.

slope = 1.34 ± 0.32; n = 3; Supplemental Fig. 2C). SPM-354 had a margin of selectivity of 1840-fold versus S1P$_2$, 8000-fold versus S1P$_4$, and 20,000-fold versus S1P$_5$ for inhibiting S1P–β-arrestin activation. SPM-354 was chosen for in vivo studies over SPM-242 due to its improved stability in vivo (the half-life in a mouse is 6.7 hours, Y. Kohno, personal communication), and allowed for a more effective in vivo probe of S1P$_3$ function.

Role for S1P$_3$ in Regulating Cardiac Rate and Rhythm In Vivo. First-dose FTY720 administration in humans is known to reduce heart rate and, in some cases, induce acute episodes of AV block (Vargas and Perumal, 2013). To further understand the contribution of S1P$_3$ in cardiac rhythm, we employed a surface ECG analysis under Avertin anesthesia in conjunction with FTY720 and SPM-354. Avertin was chosen because it is well tolerated in mice (Roth et al., 2002; Chu et al., 2006) and allowed for the capture of high-quality ECG waveforms. The heart rate plots show that administration of FTY720 to WT mice 5 hours prior to anesthesia produced significant bradycardia in all animals (n = 7; P = 0.0006; Fig. 1B, top graph, red tracing) compared with water vehicle treatment (n = 6; blue tracing). FTY720-induced bradycardia in WT mice was calculated from the RR interval on the ECG and showed a significantly increased PR-interval duration from 49 ± 3 milliseconds at baseline to 70 ± 3 milliseconds after FTY720 treatment (P = 0.0023; Fig. 1C), indicative of first-degree heart block. In contrast, and as expected (Forrest et al., 2004; Sanna et al., 2004), there were no measurable heart rate or ECG changes in KO mice treated with 20 mpk FTY720 (Fig. 1B, bottom graph, red tracing; Fig. 1D), despite KO mice having a similar heart rate modulation maxima versus WT mice following acute sympathetic and parasympathetic drug challenges (Supplemental Fig. 3).

Additional experiments with the selective S1P$_1$ agonist CYM-5442, which has therapeutic efficacy in the experimental autoimmune encephalomyelitis models of multiple sclerosis (Gonzalez-Cabrera et al., 2008, 2012) produced no bradycardia when measured 5 hours following 10 mpk i.p. administration (n = 5; Fig. 1B, green tracing).

FTY720-induced bradycardia in WT mice was fully reversed in a bimodal fashion by the i.p. bolus injection of 40 mpk SPM-354 (P = 0.001; Fig. 1B, red tracing, light arrows), but not by 40 mpk i.p. injection of the S1P$_1$ antagonist W146 (n = 5; Supplemental Fig. 4). Furthermore, reversal of bradycardia by SPM-354 administration was associated with a partial, but not significant, restoration of PR-interval elevation by FTY720 at the protocol's end (P = 0.17; Fig. 1C). Parallel studies indicated that antagonist vehicle i.p. administration in FTY720 bradycardiac mice did not alter heart rate

throughout the conditions (P = 0.148; n = 6; Fig. 1B, top graph, dark arrows), and, importantly, 40 mpk SPM-354 treatment alone did not affect the basal heart rate (P = 0.090; n = 4; Fig. 1, blue line, light arrow), even when dosed up to 120 mpk (data not shown).

To our surprise, because mice are not known to be a highly arrythmogenic species (Boukens et al., 2014) and because no descriptions of this FTY720 effect have been published, ~25% of the mice receiving FTY720/Avertin developed signs of CHB, which were characterized by prolonged periods of at least three consecutive P-waves in the absence of a propagated QRS ventricular conduction complex (ECG tracings, time point i; Fig. 2, B and C). This indicates that atrial depolarization remains intact but does not propagate through the AVN His-Purkinje fibers to depolarize the ventricle. All the mice that underwent CHB (N = 11) also displayed profound bradycardia [102 ± 30 beats per minute (bpm)] prior to establishment of CHB. Importantly, in mice with established CHB, i.p. administration of 80 mpk SPM-354 (n = 4; Fig. 2C), but not 1 mpk of atropine (n = 5; Fig. 2B), after the onset of CHB led to acute rescue of QRS ventricular conduction within the first minute and coupling to the atrial P-wave and restoration of sinus rhythm within 2–3 minutes (bottom ECG tracing). SPM-354 reversal of CHB was accompanied by a positive chronotropic response, which averaged 370 ± 28 bpm at the end of the protocol. Mice administered with atropine, on the other hand, sustained deep bradycardia (85 ± 55 bpm at the protocol's end) and CHB throughout the entire protocol. Moreover, β-cyclodextrin (vehicle) administration in two mice undergoing CHB failed to revert the abnormal ECG to the normal sinus rhythm (not shown).

$S1P_3$ Expression in the Mouse Cardiac Conduction System. We postulated that the appearance of CHB was a direct consequence of S1P- to $S1P_3$-mediated inhibition of ventricular conduction; therefore, we examined $S1P_3$ expression in cardiac tissues of KI mice by IHC confocal microscopy. Wild-type mouse $S1P_3$ was homologously replaced by KI of the coding sequence of mCherry to the immediate 3′ end of the *S1pr3* gene (Supplemental Fig. 5). Homozygous KI mice were viable and fertile and shown to express full-length $S1P_3$-mCherry in whole heart lysates by Western blot when probed with a monoclonal anti-mCherry antibody (Supplemental Fig. 6A) and become lymphopenic to acute FTY720 treatment (Supplemental Fig. 6C).

For IHC studies, we used the HCN4 antibody to the cyclic nucleotide gated K channel since it selectively labels all components of the CCS in the adult mouse heart (Yamamoto et al., 2006; Harzheim et al., 2008; Kuratomi et al., 2009; Baruscotti et al., 2011). A confocal low power view of a KI heart stained with anti-mCherry antibody for $S1P_3$ (red), HCN4 (green), and nuclei (blue) is shown in Fig. 3A, with fields for subsequent high power imaging boxed (Supplemental Fig. 7 includes the high magnification panels of Fig. 3A). Representative merged confocal images of SAN and AVN are shown (Fig. 3B) together with associated differential interference images (Supplemental Fig. 8 includes the high magnification panels of Fig. 3B). The central artery of the SAN is readily seen (a, Fig. 3B), with arterial smooth muscle expressing

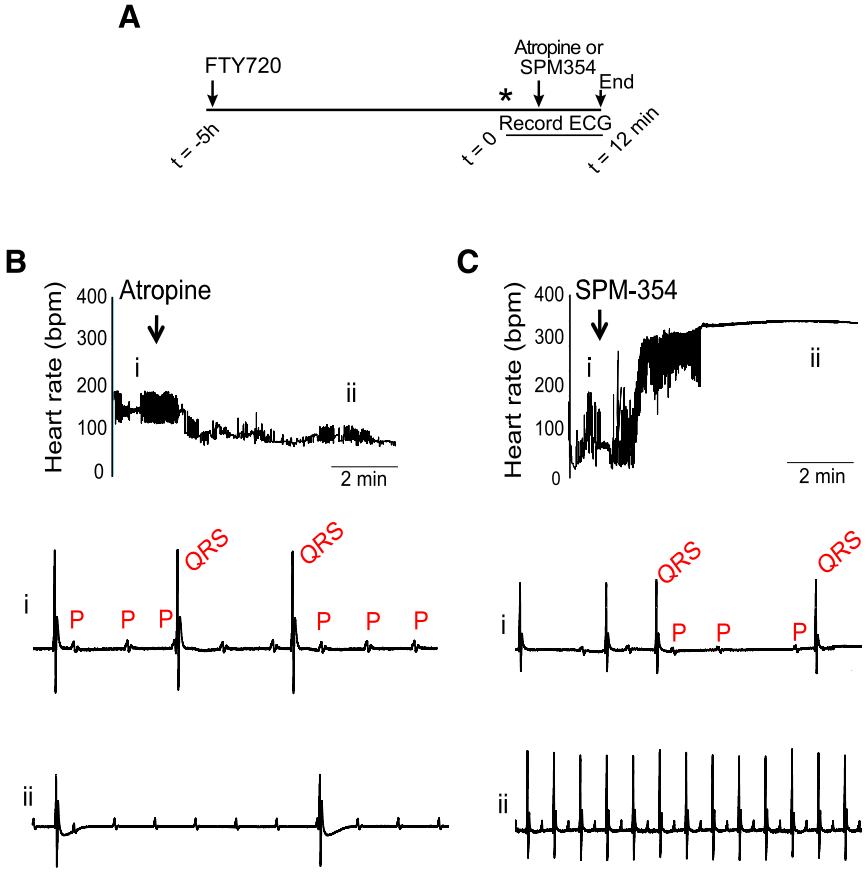

Fig. 2. FTY720 treatment increases the susceptibility for developing CHB. Typical heart rate recordings and detailed ECGs of wild-type mice undergoing CHB following 5 hours of 20 mpk FTY720 administration and anesthesia. (A) Protocol design. Single-dose 120 mpk SPM-354 administration (C), but not atropine (B), at the onset of CHB results in rapid reversal of FTY720-induced CHB within minutes. Detailed ECG analysis of mice undergoing FTY720-induced CHB has characteristic consecutive P-waves with absent QRS complexes. Representative ECG waveforms in FTY720-treated mice who received either SPM-354 or atropine while undergoing CHB. Same animal ECG recordings indicate the presence of CHB in both mice at time (i), and the outcome on cardiac rhythm post–drug treatment (ii).

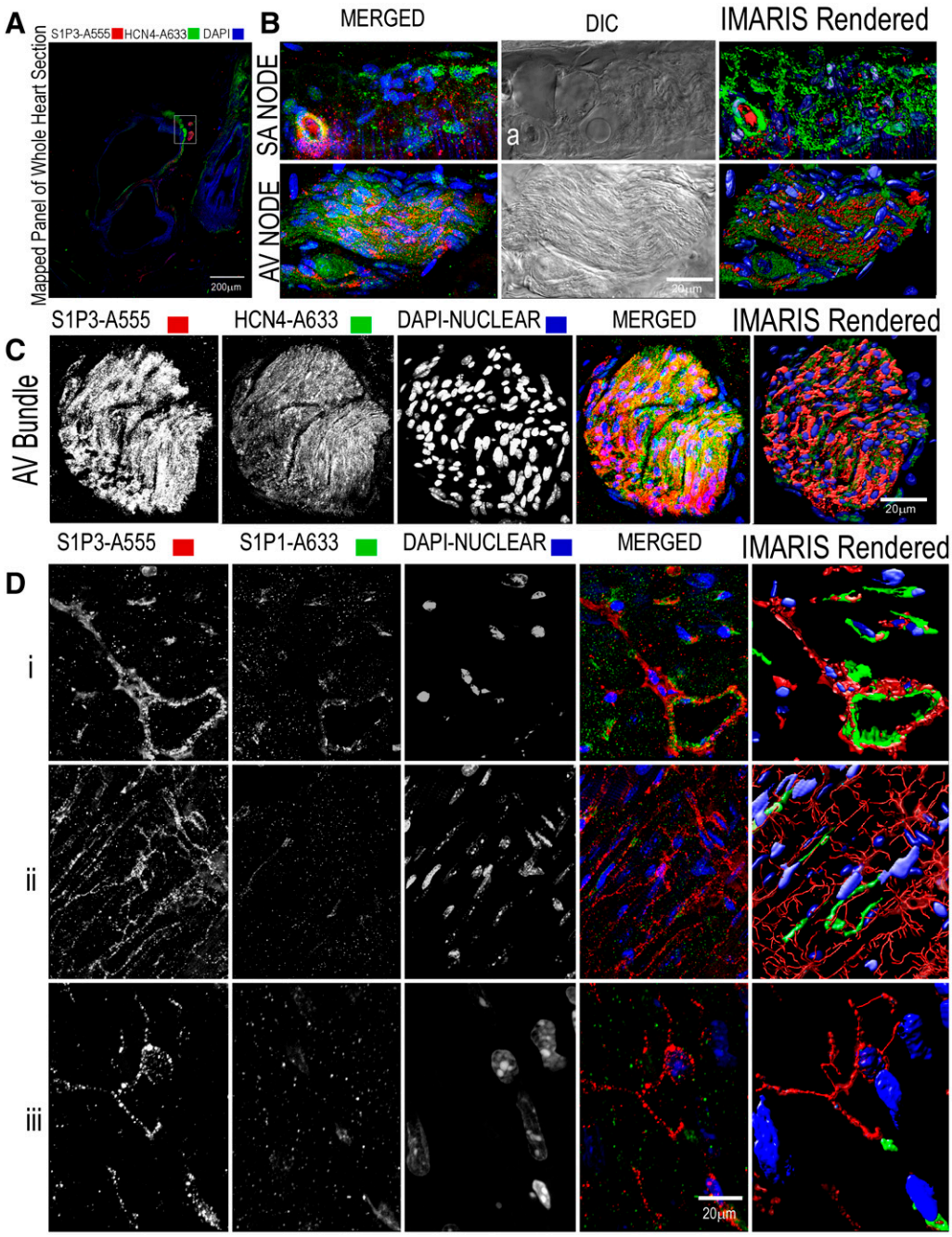

Fig. 3. Immunohistology of S1P$_3$-mCherry in the mouse cardiac conduction system. Laser scanning confocal fluorescence images and differential interferences (DICs) of whole heart, coronary artery, septum, and Purkinje fibers of S1P$_3$-mCherry KI mouse. (A) Mapped and multistitched composite of a typical whole heart section (10× objective, 40 panels) stained for S1P$_3$ (anti-mCherry/Alexa555, red), the cyclic nucleotide-gated K+ channel 4 (HCN4) (green), and nuclei (DAPI-nuclear, blue). Signals strongly positive for S1P$_3$-mCherry and HCN4 are clearly evident in the Purkinje-conduction system, as indicated in the white rectangle box of the image. (B) Examples of high-resolution multistack and maximum projected confocal images (63×) of the SA and AV nodes are shown as both merged fluorescence and DIC image projections. S1P$_3$ (red) is significantly less expressed with HCN4 in the SA node and strongly expressed in the AV node. Nuclei are shown in blue, and the sinoatrial nodal artery is indicated (a). The IMARIS-rendered images are also shown on the right panels. (C) Cross section of the AV bundle labeled with the same antibodies as in (A and B). (D) S1P$_3$ is localized in Purkinje fibers and in smooth muscle of the S1P$_3$-mCherry KI mouse heart. Panels show high-resolution (63×) multistack and maximum projected laser scanning confocal fluorescence images of cardiac smooth muscle cells (i) and Purkinje fibers (ii and iii), labeled with S1P$_3$ (anti-mCherry/Alexa555, red), S1P$_1$ (anti-GFP/Alexa633, green), and nuclei (DAPI, blue). S1P$_3$ is expressed in heart coronary artery smooth muscle and Purkinje fibers, whereas S1P$_1$ is localized in the endothelium (i). The last panel series following the merged image shows a single snap shot image of a three-dimensional surface-rendered reconstruction of the fluorescent signals created with the IMARIS software. Longitudinal sections of heart ventricular septum (ii) shows S1P$_3$ (red) staining of heart Purkinje fibers as projections interdigitating between ventricular myocytes. A magnified image (iii) of a single Purkinje fiber further shows axonal-like projections wrapped around myocytes.

S1P$_3$-mCherry. Obvious HCN4 staining of SAN is seen with a small number of interdigitating S1P$_3$-mCherry positive processes. The atrioventricular node shows a characteristic morphology on differential interference and is strongly double positive for both S1P$_3$-mCherry and HCN4 (see Supplemental Fig. 8 for relative quantification of HCN4 and mCherry

merged images in AVN and SAN). The bundle of His, shown in the cross section in Fig. 3C, is also strongly double labeled for both HCN4 and $S1P_3$-mCherry (a three-dimensional isosurfacing IMARIS image is shown on the rightmost panel of Fig. 3C). Additional IHC experiments using left ventricle heart sections from double-cross, $S1P_1$-GFP × $S1P_3$-mCherry, homozygous KI mice, showed $S1P_3$-mCherry expression (red) in Purkinje fibers as projections interdigitating between ventricular myocytes and coronary artery smooth muscle (Fig. 3D, panel ii). A magnified image of a single Purkinje fiber further shows axonal-like projections wrapped around myocytes (Fig. 3D, panel iii). In contrast, $S1P_1$-GFP expression was, as expected (Cahalan et al., 2011), predominantly found on vascular endothelium (Fig. 3D, panel i). mCherry positive projections could be double labeled with anti-mCherry mAb and Pan-neuronal markers (Supplemental Fig. 9C), supporting the neuronal origin of $S1P_3$ projections and their identification as Purkinje fibers. In addition, and as reported (Mazurais et al., 2002; Forrest et al., 2004), we found strong discrete $S1P_3$-mCherry expression in vascular smooth muscle, which was differentiated from endothelial cells, as shown in samples colabeled with the endothelial marker CD31 (Supplemental Fig. 9, A and B).

Incidence of FTY720-Induced CHB Can Be Increased to Almost 100% by Propranolol Administration. To assay the FTY720-induced CHB phenotype with a more robust protocol, we included the nonselective β-androgen receptor antagonist propranolol, which is known to reduce heart rate and cardiac output in mice. FTY720-induced CHB was demonstrated by administering both FTY720 and propranolol, as shown in Fig. 4A. Under this protocol, we studied the actions of vehicle or SPM-354 administration 2 minutes prior to anesthesia. The establishment of CHB in FTY720/propranolol-treated WT mice with β-cyclodextrin vehicle preadministration prior to anesthesia increased to almost 100% (eight out of nine mice displayed CHB throughout the protocol; Table 1) and was associated with consistently low heart rates, usually below 100 bpm, as represented in the red tracing (Fig. 4B). In parallel experiments, intraperitoneal injection of SPM-354 (120 mpk) 2 minutes prior to anesthesia

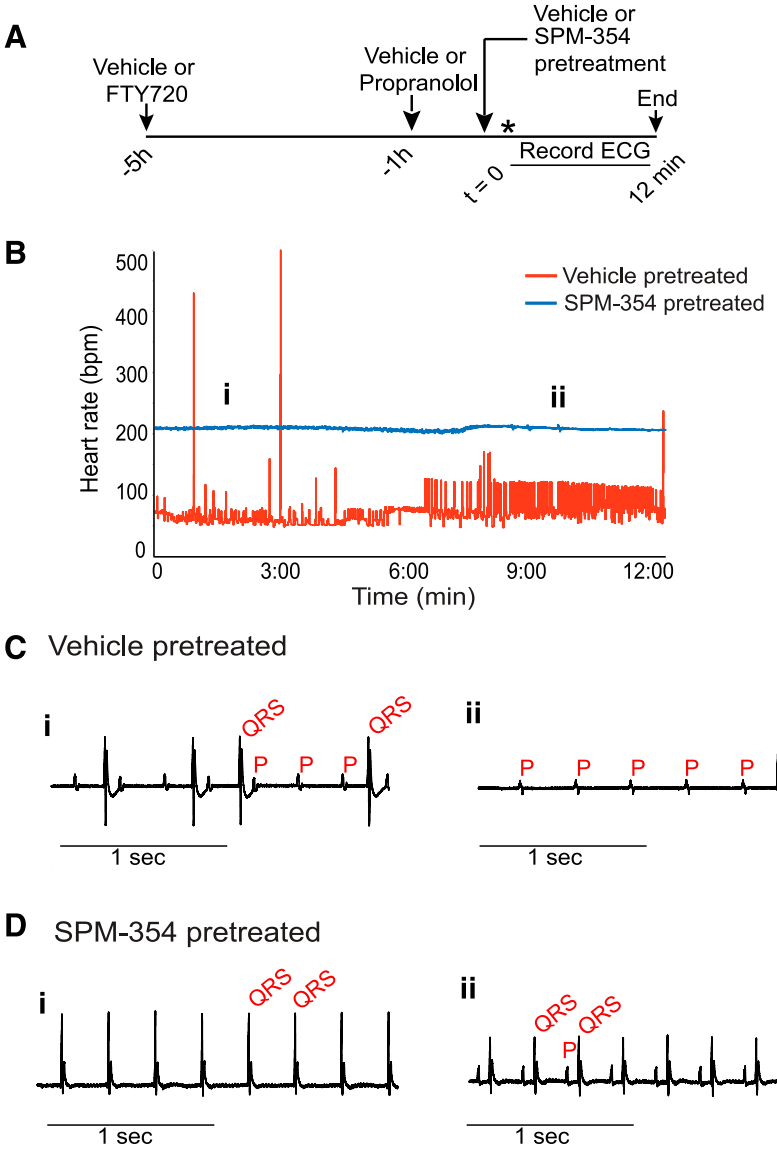

Fig. 4. The incidence of FTY720-induced CHB increased by propranolol coadministration requires $S1P_3$ and is reversed by single-dose SPM-354 administration. (A) Protocol schema. (B) Representative heart rate recordings with magnified sections of the ECG at times (i) and (ii) of the recordings in mice administered with FTY720/propranolol and acutely pretreated with either vehicle (red tracing) or SPM-354 (blue tracing) 2 minutes prior to anesthesia. Vehicle-pretreated, FTY720/propranolol mice displayed deep bradycardia and an irregular heart rate throughout and had distinctive CHB episodes characteristic of consecutive P-waves with skipped QRS complexes (C). In comparison, SPM-354 pretreated, FTY720/propranolol mice displayed a steady heart rate, with no signs of CHB, as depicted in the magnified ECG taken at times (i) and (ii) of the recording (D). Table 1 includes the number of WT, $S1P_3$ KO, and $S1P_3$ KI mice that underwent CHB under the protocol diagrammed in (A), the mean ± S.E.M. heart rates at the protocol's end, and the outcome of vehicle and/or SPM-354 administration on CHB establishment.

TABLE 1
Incidence of CHB and heart rates from in vivo FTY720 and propranolol administration in WT, KI, and KO mice acutely pretreated with either vehicle or SPM-354

Treatment Group	FTY720 + Propranolol[a]			
	Vehicle[b]		SPM-354[b]	
	Number of Mice without CHB (Mice Tested)	Heart Rate	Number Mice without CHB (Mice Tested)	Heart Rate
		bpm		*bpm*
Wild type	1 (9)	N.D.	7 (8)	219 ± 12
Knockin	2 (7)	N.D.	4 (4)	148 ± 7.0
Knockout	5 (5)	350 ± 6.0	N.D.	N.D.

N.D., not determined.
[a]4 hours and 1 hour, respectively.
[b]Acute 2-minute pretreatment.

to WT mice with FTY720-propranolol nearly completely prevented the establishment of CHB (seven out of eight mice studied; Table 1) by maintaining sinus rhythm and an adequate heart rate, as evidenced from the ECG pattern of SPM-354–pretreated mice relative to vehicle (Fig. 4, C and D). Table 1 shows that when this protocol was applied to KO mice, there were no signs of CHB in the ECG ($N = 5$), although KO mice were slightly bradycardic due to propranolol administration. No differences in heart rate were noted to the administration of vehicles between WT and KO mice (WT baseline: 458 ± 12; WT end of the recording: 443 ± 8; KO baseline: 445 ± 17; KO end of recording: 423 ± 10). The FTY720 induction of nonlethal bradycardia and its reversal by SPM-354 (Supplemental Fig. 6B) as well as SPM-354 prevention of FTY720-propranolol induced CHB (Table 1) were also demonstrated in the $S1P_3$ KI mice, providing formal evidence for the normal pharmacological function of the tagged receptor KI.

SPM-354 Reverses S1P-Induced Normal ECG Function and S1P-Induced CHB in Isolated, Perfused Hearts. To differentiate between central or peripheral actions of SPM-354 CHB reversal in vivo, direct effects on cardiac rate and rhythm were studied in Langendorff preparations, with S1P as the ligand. For these studies, we tracked both the RR-interval duration along with modulation of the CF rate by the drugs, the latter serving as an internal control of S1P-$S1P_3$ function and antagonist reversal (Murakami et al., 2010). We found that perfusion of increasing concentrations of S1P to isolated WT hearts reduced CF rate in a concentration-dependent manner (Supplemental Fig. 10, A and B; $N = 4$; EC_{50} of 0.80 ± 0.14 μM), which amounted to a 4.4-fold reduction of 80% maximal response versus baseline CF rate (Table 2; normal ECG values). According to previous reports of S1P-$S1P_3$ mediated coronary vasoconstriction (Murakami et al., 2010), a subsequent bolus of 3 μM SPM-354 during maximal 10 μM S1P CF rate reduction led to rapid reversal toward the baseline CF rate and, in some cases, to above-baseline values (Supplemental Fig. 10A). Complete tracking of the RR-interval duration in Supplemental Fig. 10A shows that at 3 μM S1P, there is a sharp increase in the RR-interval duration, accompanied by segments of high interbeat variability, which appeared sustained at 10 μM S1P, and, like CF, were rapidly reversed to baseline values following 3 μM SPM-354 perfusion (Table 2; normal ECG values).

TABLE 2
SPM-354 reverses S1P-induced RR interval augmentation and S1P-mediated CFR reduction in isolated perfused hearts of WT mice undergoing either normal ECG patterns or those displaying CHB
Baseline values were taken immediately following 5 minutes of heart equilibration from start of perfusion.

Treatment	Normal ECG		CHB	
	RR Interval	CFR	RR Interval	CFR
	milliseconds	*ml/min*	*milliseconds*	*ml/min*
Baseline	177 ± 35	1.31 ± 0.31	168 ± 7.6	1.33 ± 0.40
+ S1P	351 ± 164*	0.27 ± 0.15*	620 ± 177**	0.25 ± 0.05*
+ SPM-354	156 ± 42[a]	1.32 ± 0.86[a]	205 ± 31***	1.65 ± 0.54[a]

[a]Not significant versus baseline.
*$P < 0.05$ versus baseline.
**$P < 0.01$ versus baseline.
***$P < 0.05$ versus S1P.

Further analysis into S1P perfusion and cardiac rhythm variability was done using 3 μM S1P or an approximate EC_{80} of the S1P-mediated reduction in the CF rate. In the Langendorff, S1P-induced arrhythmias are readily seen (Fig. 5A), with the sequential transition from normal sinus rhythm at baseline to gradual and steady bradycardia (not shown), then second-degree heart blocks with 2:1 and 3:1 atrioventricular conduction (S1P), and finally to CHB, as shown by a complete absence of QRS ventricular complexes. Figure 5A (vehicle) demonstrates that vehicle perfusion to a heart with complete absence of QRS ventricular complexes does not induce reversal to normal rhythm, unlike subsequent perfusion with 3 μM SPM-354 (end of tracing in Fig. 5A). Moreover, acute CHB (QRS complex suppression) following 3 μM S1P perfusion was atropine resistant (Fig. 5B); in contrast, in all three examples shown, perfusion with 3 μM SPM-354 reverted the isolated CHB to sinus rhythm, which was accompanied by both compensatory tachycardia and restoration of the CF rate to near baseline values (end of tracing in Fig. 5B; Table 2; CHB values).

To formally exclude a role for $S1P_1$ in the CHB phenotype, additional experiments tested the effects of $S1P_1$ antagonist W146 perfusion on S1P-induced CHB in WT hearts (Fig. 5C). The data show that in established 3 μM S1P-induced CHB, W146 perfusion at 10 μM does not modify the abnormal cardiac rhythm, whereas subsequent SPM-354 perfusion at 3 μM fully restored CHB to a normal, steady waveform ECG in all four hearts studied.

To conclude that S1P-induced CHB was dependent on $S1P_3$, we performed Langendorff experiments in hearts from $S1P_3$ KO mice (Supplemental Fig. 11). Unlike WT (Supplemental Fig. 11A), bolus perfusion of 3 μM S1P to KO hearts (Supplemental Fig. 11B) produced marginal elevations in the RR-interval duration throughout the protocol, and, despite inducing modest, albeit significant 30% acute inhibition in the CF rate (Supplemental Fig. 11C), S1P did not elicit measurable cardiac arrhythmias or CHB in KO hearts ($n = 7$).

Discussion

This combination of genetic and pharmacological analyses in WT, receptor KO, and KI mice provides multiple lines of evidence for S1P receptor subtype selective differential regulation of atrial and ventricular pacemaking and conduction events. $S1P_1$ has been shown to regulate sinus bradycardia, is coupled to G protein-coupled inwardly-rectifying potassium

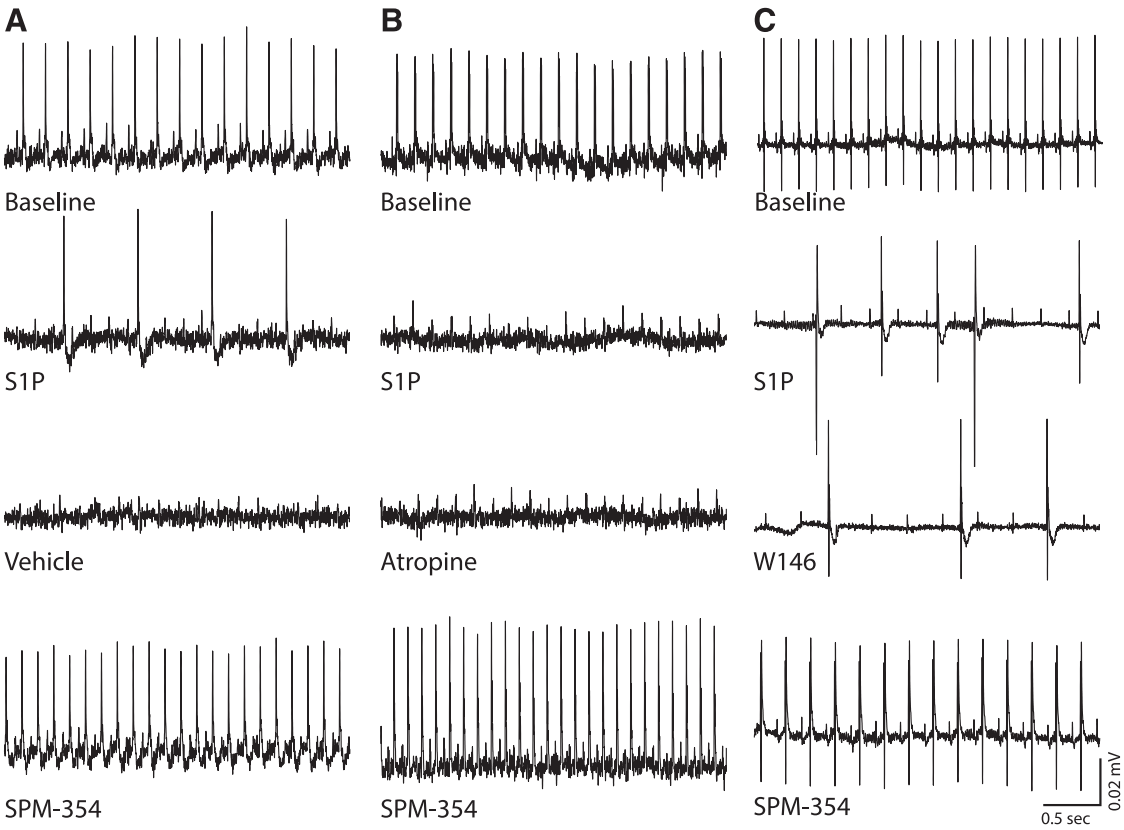

Fig. 5. SPM-354 reverses S1P-induced CHB in ex vivo mouse heart studies. Volume-conducted ECGs were measured in isolated, unpaced, Langendorff-perfused WT mouse hearts under constant pressure. The four rows for each panel contain representative 3-second ECG tracings shown at baseline, 3 minutes following a bolus of 3 μM S1P, 3 minutes following a bolus of vehicle/W146, and 3 minutes following a bolus of SPM-354. After S1P introduction, baseline sinus rhythm (A–C; top row) degenerates into second-degree AV block with a variable RR interval and eventually CHB (A and B; second row). β-cyclodextrin vehicle (A; third row), 1 μM atropine (B; third row), and 10 μM W146 (C; third row) fail to rescue S1P-induced CHB, whereas SPM-354 (A–C; bottom row) restores AV conduction and returns the heart to a normal sinus rhythm.

channel (Guo et al., 1999), and is responsible for the atropine sensitive vagal sinus bradycardia (Kovarik et al., 2008; Fryer et al., 2012; Legangneux et al., 2013). $S1P_3$ in mice has rich expression at the mRNA level on cells of neural crest origin (Meng and Lee, 2009) and was recently shown to be transcriptionally present along *S1pr1* and *S1pr2* transcripts in the AVN of rats. We corroborate this finding in the KI mouse and find expression of $S1P_3$-mCherry on neural crest–derived AVN, His bundles, and cardiac Purkinje fibers in addition to finding a relatively high expression, as expected, on vascular smooth muscle in the coronary arteries (Forrest et al., 2004).

In mice, $S1P_3$ agonism by FTY720-P as well as the chiral analog 2-amino-4-(4-(heptyloxy)-phenyl)-2-methylbutyl dihydrogen phosphate produce bradycardia in WT, but not in $S1P_3$-deletant, mice (Forrest et al., 2004; Sanna et al., 2004). Based on the KI IHC findings and using proof-of-concept reversal of FTY720 bradycardia, we characterized a potent $S1P_3$ antagonist tool, SPM-354, to further query physiologic functions of cardiac $S1P_3$ modulation.

We confirmed that FTY720 does not induce bradycardia in KO mice, whereas in bradycardic WT and/or KI mice pre-administered with FTY720, single-dose SPM-354 induced a significant positive, chronotropic response, as shown previously by Murakami et al. (2010) with a separate $S1P_3$ antagonist.

Most importantly, we show the first evidence of FTY720's arrythmogenic potential in anesthetized WT mice, particularly in those mice experiencing severe bradycardia (<200 bpm) due to FTY720 coadministration along with the beta-blocker propranolol. Cardiac arrhythmias induced by FTY720-propranolol treatment in WT mice included episodes of CHB, where AV propagation of atrial depolarization is absent. Notably, 2-minute prior treatment with single-dose SPM-354 in FTY720-propranolol pretreated WT and/or KI mice largely prevented the establishment of CHB, while maintaining a fairly constant heart rate, albeit a low (approximately 200 bpm) and normal rhythm, throughout the protocol.

Lack of arrhythmias in $S1P_3$-KO mice by FTY720-propranolol, coupled with the high $S1P_3$ IHC expression in mouse CCS and prevention of CHB by the $S1P_3$ antagonist SPM-354 in WT and KI mice, provide support that arrythmogenesis is strongly dependent on cardiac-intrinsic $S1P_3$ agonism. However, in vivo limitations of the study precluding absolute interpretation of the "origin" of the FTY720-induced conduction defects include: 1) possible modulation of other cardiac receptors (the mouse heart expresses $S1P_1$, $S1P_2$, and $S1P_5$); 2) the known FTY720-mediated $S1P_3$ bronchoconstriction in mice, as shown by Trifilief and Fozard (2012), which would be relevant and potentially aggravated by coadministration of the nonselective beta-blocker propranolol; and 3) use of an anesthetic.

The potential limitations are solved by measuring the cardiac rate and rhythm directly in isolated hearts. We chose

S1P for the Langendorff hung heart studies rather than prodrug FTY720 to avoid fingolimod's intrinsic requirement for kinase phosphorylation by sphingosine kinase-2 to become an active agonist of $S1P_3$ and remove any potential for off-target effects of FTY720, such as sphingosine-1-phosphate lyase (Bandhuvula et al., 2005) and Transient receptor potential melastatin 7 (Qin et al., 2013). These Langendorff studies provide the first evidence for direct $S1P_3$ cardiac intrinsic induction of lethal cardiac arrhythmias, including CHB, which are highly sensitive to reversal by the $S1P_3$ antagonist SPM-354. To add validation to SPM-354 as an antagonist of $S1P_3$ with 30-fold higher potency over $S1P_1$, we measured CF rate reduction by $S1P_3$ agonism and reversal thereof by SPM-354 since the S1P-$S1P_3$ axis reduces the CF rate via coronary vasoconstriction. The data indicate that S1P-induced arrhythmias presented sporadically, whereas CF rate reduction maxima and RR-interval elevation functions of S1P were universal. Moreover, SPM-354, and not the $S1P_1$ antagonist W146, fully reversed all three functions of S1P perfusion, whereas CHB was atropine insensitive and rapidly reversed by SPM-354, as similarly observed in the reversal of CHB with FTY720 in vivo.

Ischemia is not likely a significant factor in S1P-induced CHB. Specifically, we found that S1P infusion did not stop CF (E_{max} = 0.80), allowing maintenance of residual constant pressure perfusion. In contrast, global ischemia models of arrhythmia require complete inhibition of CF for prolonged periods of 10 minutes or more. The onset of CHB in response to S1P or FTY720 and propranolol is very rapid (Fig. 4), and SPM-354–initiated recovery from acute CHB is equally rapid. Electrocardiographic evidence shows that SPM-354 first initiates an idioventricular rhythm in the first 60 seconds after infusion, followed by full coupling into the sinus rhythm by minute 2. These ECG data support a direct effect on ventricular pacemaking cells and the rapidity of recovery reflects a very effective and rapid perfusion of the ventricles in the face of CHB.

SPM-354 fits the definition of a bitopic ligand for $S1P_3$ based upon receptor kinetic studies. SPM-354 can compete for the published allosteric $S1P_3$ selective agonist CYM-5541 (Schuerer et al., 2008; Jo et al., 2012) as well as for the orthosteric agonist S1P, whereas CYM-5541 is unable to compete for the binding of the orthosteric S1P ligand (Jo et al., 2012). SPM-354 was chosen for in vivo studies over the previously described SPM-242 ligand because it has improved in vivo efficacy. This stems from its 6- to 10-fold improvement in the apparent K_i as an $S1P_3$ antagonist, for which the (*S*)-enantiomer is essential to avoid agonism. In addition, SPM-242 with is 2-hydroxymethyl substituent underwent very rapid phosphate ester hydrolysis in vivo, whereas the 2-propyl substituent in SPM-354 slows down the susceptibility to phosphohydrolases and enhances the half-life and persistence of SPM-354, allowing it to be a more effective in vivo probe of $S1P_3$ function.

In summary, modulation of $S1P_3$ activity is causally associated with AV nodal conduction block from three lines of evidence. First, $S1P_3$ must be present for the induction of cardiac conduction changes by FTY720 and S1P as deletion of *S1pr3* leads to mice being refractory to these agonist-induced changes. Second, the $S1P_3$ antagonist SPM-354 attenuates the failure of ventricular activation in nearly all mice, with ECG signs of CHB by the beta-blocker propranolol and FTY720 coadministration, and restores normal sinus rhythm. Third, S1P-induced CHB is replicated in Langendorff preparations and reversed by SPM-354 and not atropine or the $S1P_1$ antagonist W146.

$S1P_3$ distribution in the mouse heart thus provides an insight into a potential mechanism-based cardiac risk that now prompts verification of $S1P_3$ expression in the human CCS. These new insights into $S1P_3$ usage in the pacemaker cells of the mouse heart will enhance understanding of ventricular conduction physiology and pathology, particularly as pharmacological tools allow these data to be extended into larger animal species and humans.

Authorship Contributions

Participated in research design: Rosen, Gonzalez-Cabrera, Sanna, Repetto, Cahalan, J. Brown, McCulloch, Vincent.

Conducted experiments: Gonzalez-Cabrera, Vincent, Sanna, Repetto, Kiosses, S. Brown, Abgaryan, Riley, Leaf, Nguyen.

Contributed new reagents or analytic tools: Kohno, McCulloch.

Performed data analysis: Gonzalez-Cabrera, Vincent, Sanna, Kiosses, S. Brown, Abgaryan, Riley.

Wrote or contributed to the writing of the manuscript: Rosen, Gonzalez-Cabrera, Sanna, Vincent, S. Brown.

References

Bandhuvula P, Tam YY, Oskouian B, and Saba JD (2005) The immune modulator FTY720 inhibits sphingosine-1-phosphate lyase activity. *J Biol Chem* **280**: 33697–33700.

Baruscotti M, Bucchi A, Viscomi C, Mandelli G, Consalez G, Gnecchi-Rusconi T, Montano N, Casali KR, Micheloni S, and Barbuti A et al. (2011) Deep bradycardia and heart block caused by inducible cardiac-specific knockout of the pacemaker channel gene Hcn4. *Proc Natl Acad Sci USA* **108**:1705–1710.

Boukens BJ, Rivaud MR, Rentschler S, and Coronel R (2014) Misinterpretation of the mouse ECG: 'musing the waves of Mus musculus'. *J Physiol* **592**:4613–4626.

Bunemann M, Brandts B, zu Heringdorf DM, van Koppen CJ, Jakobs KH, and Pott L (1995) Activation of muscarinic K+ current in guinea-pig atrial myocytes by sphingosine-1-phosphate. *J Physiol* **489**:701–777

Cahalan SM, Gonzalez-Cabrera PJ, Sarkisyan G, Nguyen N, Schaeffer MT, Huang L, Yeager A, Clemons B, Scott F, and Rosen H (2011) Actions of a picomolar short-acting $S1P_1$ agonist in $S1P_1$-eGFP knock-in mice. *Nat Chem Biol* **7**:254–256.

Chu DK, Jordan MC, Kim JK, Couto MA, and Roos KP (2006) Comparing isoflurane with tribromoethanol anesthesia for echocardiographic phenotyping of transgenic mice. *J Am Assoc Lab Anim Sci* **45**:8–13.

Cohen JA, Barkhof F, Comi G, Hartung HP, Khatri BO, Montalban X, Pelletier J, Capra R, Gallo P, and Izquierdo G et al.; TRANSFORMS Study Group (2010) Oral fingolimod or intramuscular interferon for relapsing multiple sclerosis. *N Engl J Med* **362**:402–415.

Egom EE, Kruzliak P, Rotrekl V, and Lei M (2015) The effect of the sphingosine-1-phosphate analogue FTY720 on atrioventricular nodal tissue. *J Cell Mol Med* **19**: 1729–1734.

Espinosa PS and Berger JR (2011) Delayed fingolimod-associated asystole. *Mult Scler* **17**:1387–1389.

Forrest M, Sun SY, Hajdu R, Bergstrom J, Card D, Doherty G, Hale J, Keohane C, Meyers C, and Milligan J et al. (2004) Immune cell regulation and cardiovascular effects of sphingosine 1-phosphate receptor agonists in rodents are mediated via distinct receptor subtypes. *J Pharmacol Exp Ther* **309**:758–768.

Fryer RM, Muthukumarana A, Harrison PC, Nodop Mazurek S, Chen RR, Harrington KE, Dinallo RM, Horan JC, Patnaude L, and Modis LK et al. (2012) The clinically-tested S1P receptor agonists, FTY720 and BAF312, demonstrate subtype-specific bradycardia ($S1P_1$) and hypertension ($S1P_3$) in rat. *PLoS One* **7**: e52985.

Gonzalez-Cabrera PJ, Cahalan SM, Nguyen N, Sarkisyan G, Leaf NB, Cameron MD, Kago T, and Rosen H (2012) S1P(1) receptor modulation with cyclical recovery from lymphopenia ameliorates mouse model of multiple sclerosis. *Mol Pharmacol* **81**: 166–174.

Gonzalez-Cabrera PJ, Jo E, Sanna MG, Brown S, Leaf N, Marsolais D, Schaeffer MT, Chapman J, Cameron M, and Guerrero M et al. (2008) Full pharmacological efficacy of a novel S1P1 agonist that does not require S1P-like headgroup interactions. *Mol Pharmacol* **74**:1308–1318.

Guo J, MacDonell KL, and Giles WR (1999) Effects of sphingosine 1-phosphate on pacemaker activity in rabbit sino-atrial node cells. *Pflugers Arch* **438**:642–648.

Hanson MA, Roth CB, Jo E, Griffith MT, Scott FL, Reinhart G, Desale H, Clemons B, Cahalan SM, and Schuerer SC et al. (2012) Crystal structure of a lipid G protein-coupled receptor. *Science* **335**:851–855.

Harzheim D, Pfeiffer KH, Fabritz L, Kremmer E, Buch T, Waisman A, Kirchhof P, Kaupp UB, and Seifert R (2008) Cardiac pacemaker function of HCN4 channels in mice is confined to embryonic development and requires cyclic AMP. *EMBO J* **27**: 692–703.

Ishii I, Friedman B, Ye X, Kawamura S, McGiffert C, Contos JJ, Kingsbury MA, Zhang G, Brown JH, and Chun J (2001) Selective loss of sphingosine 1-phosphate signaling with no obvious phenotypic abnormality in mice lacking its G protein-coupled receptor, LP(B3)/EDG-3. *J Biol Chem* **276**:33697–33704.

Jo E, Bhhatarai B, Repetto E, Guerrero M, Riley S, Brown SJ, Kohno Y, Roberts E, Schürer SC, and Rosen H (2012) Novel selective allosteric and bitopic ligands for the S1P(3) receptor. *ACS Chem Biol* **7**:1975–1983.

Kappos L, Radue EW, O'Connor P, Polman C, Hohlfeld R, Calabresi P, Selmaj K, Agoropoulou C, Leyk M, and Zhang-Auberson L et al.; FREEDOMS Study Group (2010) A placebo-controlled trial of oral fingolimod in relapsing multiple sclerosis. *N Engl J Med* **362**:387–401.

Kovarik JM, Slade A, Riviere GJ, Neddermann D, Maton S, Hunt TL, and Schmouder RL (2008) The ability of atropine to prevent and reverse the negative chronotropic effect of fingolimod in healthy subjects. *Br J Clin Pharmacol* **66**:199–206.

Kuratomi S, Ohmori Y, Ito M, Shimazaki K, Muramatsu S, Mizukami H, Uosaki H, Yamashita JK, Arai Y, and Kuwahara K et al. (2009) The cardiac pacemaker-specific channel Hcn4 is a direct transcriptional target of MEF2. *Cardiovasc Res* **83**:682–687.

Legangneux E, Gardin A, and Johns D (2013) Dose titration of BAF312 attenuates the initial heart rate reducing effect in healthy subjects. *Br J Clin Pharmacol* **75**: 831–841.

Liao R, Podesser BK, and Lim CC (2012) The continuing evolution of the Langendorff and ejecting murine heart: new advances in cardiac phenotyping. *Am J Physiol Heart Circ Physiol* **303**:H156–H167.

Mazurais D, Robert P, Gout B, Berrebi-Bertrand I, Laville MP, and Calmels T (2002) Cell type-specific localization of human cardiac S1P receptors. *J Histochem Cytochem* **50**:661–670.

Mendelson K, Evans T, and Hla T (2014) Sphingosine 1-phosphate signalling. *Development* **141**:5–9.

Meng H and Lee VM (2009) Differential expression of sphingosine-1-phosphate receptors 1-5 in the developing nervous system. *Dev Dyn* **238**:487–500.

Murakami A, Takasugi H, Ohnuma S, Koide Y, Sakurai A, Takeda S, Hasegawa T, Sasamori J, Konno T, and Hayashi K et al. (2010) Sphingosine 1-phosphate (S1P) regulates vascular contraction via S1P3 receptor: investigation based on a new S1P3 receptor antagonist. *Mol Pharmacol* **77**:704–713.

Parrill AL, Wang D, Bautista DL, Van Brocklyn JR, Lorincz Z, Fischer DJ, Baker DL, Liliom K, Spiegel S, and Tigyi G (2000) Identification of Edg1 receptor residues that recognize sphingosine 1-phosphate. *J Biol Chem* **275**:39379–39384.

Qin X, Yue Z, Sun B, Yang W, Xie J, Ni E, Feng Y, Mahmood R, Zhang Y, and Yue L (2013) Sphingosine and FTY720 are potent inhibitors of the transient receptor potential melastatin 7 (TRPM7) channels. *Br J Pharmacol* **168**:1294–1312.

Rosen H, Stevens RC, Hanson M, Roberts E, and Oldstone MBA (2013) Sphingosine-1-phosphate and its receptors: structure, signaling, and influence. *Annu Rev Biochem* **82**:637–662.

Roth DM, Swaney JS, Dalton ND, Gilpin EA, and Ross J, Jr (2002) Impact of anesthesia on cardiac function during echocardiography in mice. *Am J Physiol Heart Circ Physiol* **282**:H2134–H2140.

Salomone S, Potts EM, Tyndall S, Ip PC, Chun J, Brinkmann V, and Waeber C (2008) Analysis of sphingosine 1-phosphate receptors involved in constriction of isolated cerebral arteries with receptor null mice and pharmacological tools. *Br J Pharmacol* **153**:140–147.

Salomone S, Yoshimura S, Reuter U, Foley M, Thomas SS, Moskowitz MA, and Waeber C (2003) S1P3 receptors mediate the potent constriction of cerebral arteries by sphingosine-1-phosphate. *Eur J Pharmacol* **469**:125–134.

Sanna MG, Liao J, Jo E, Alfonso C, Ahn MY, Peterson MS, Webb B, Lefebvre S, Chun J, and Gray N et al. (2004) Sphingosine 1-phosphate (S1P) receptor subtypes S1P1 and S1P3, respectively, regulate lymphocyte recirculation and heart rate. *J Biol Chem* **279**:13839–13848.

Sanna MG, Wang SK, Gonzalez-Cabrera PJ, Don A, Marsolais D, Matheu MP, Wei SH, Parker I, Jo E, and Cheng WC et al. (2006) Enhancement of capillary leakage and restoration of lymphocyte egress by a chiral S1P1 antagonist *in vivo*. *Nat Chem Biol* **2**:434–441.

Schmouder R, Serra D, Wang Y, Kovarik JM, DiMarco J, Hunt TL, and Bastien MC (2006) FTY720: placebo-controlled study of the effect on cardiac rate and rhythm in healthy subjects. *J Clin Pharmacol* **46**:895–904.

Schürer SC, Brown SJ, Gonzalez-Cabrera PJ, Schaeffer MT, Chapman J, Jo E, Chase P, Spicer T, Hodder P and Rosen H (2008) Ligand-binding pocket shape differences between sphingosine 1-phosphate (S1P) receptors S1P1 and S1P3 determine efficiency of chemical probe identification by ultrahigh-throughput screening. *ACS Chem Biol* **3**:486–498.

Trifilieff A and Fozard JR (2012). Sphingosine-1-phosphate-induced airway hyperreactivity in rodents is mediated by the sphingosine-1-phosphate type 3 receptor. *J Pharmacol Exp Ther* **342**:399–406.

Vanoli E, Pentimalli F and Botto G (2014) Vagomimetic effects of fingolimod: physiology and clinical implications. *CNS Neurosci Ther* **20**:496–502.

Vargas WS and Perumal JS (2013) Fingolimod and cardiac risk: latest findings and clinical implications. *Ther Adv Drug Saf* **4**:119–124.

Yagi Y, Nakamura Y, Kitahara K, Harada T, Kato K, Ninomiya T, Cao X, Ohara H, Izumi-Nakaseko H, and Suzuki K et al. (2014) Analysis of onset mechanisms of a sphingosine 1-phosphate receptor modulator fingolimod-induced atrioventricular conduction block and QT-interval prolongation. *Toxicol Appl Pharmacol* **281**: 39–47.

Yamamoto M, Dobrzynski H, Tellez J, Niwa R, Billeter R, Honjo H, Kodama I, and Boyett MR (2006) Extended atrial conduction system characterised by the expression of the HCN4 channel and connexin45. *Cardiovasc Res* **72**:271–281.

Yang AH, Ishii I, and Chun J (2002) In vivo roles of lysophospholipid receptors revealed by gene targeting studies in mice. *Biochim Biophys Acta* **1582**:197–203.

Yasushi K, Fujii K, Taru M, and Miyoshi K (2011) inventors, Kyorin Pharmaceutical Co., Ltd, assignee. DIPHENYL SULFIDE DERIVATIVES AND MEDICINES CONTAINING SAME AS ACTIVE INGREDIENT. Patent WO/2011/004604. 2011 Jan 13.

Address correspondence to: Hugh Rosen, Department of Chemical Physiology, The Scripps Research Institute, 10550 N. Torrey Pines Rd., La Jolla, CA 92037. E-mail: hrosen@scripps.edu or Pedro J. Gonzalez-Cabrera, Department of Chemical Physiology, The Scripps Research Institute, 10550 N. Torrey Pines Rd., La Jolla, CA 92037. E-mail: gonzalp@scripps.edu